MOLECULAR AND CELLULAR BIOLOGY, June 2003, p. 3788–3797 Vol. 23, No. 11
0270-7306/03/$08.00+0 DOI: 10.1128/MCB.23.11.3788–3797.2003

Polyphosphate Loss Promotes SNF/SWI- and Gcn5-Dependent Mitotic Induction of *PHO5*

Daniel W. Neef and Michael P. Kladde*

Department of Biochemistry and Biophysics, Texas A&M University, College Station, Texas 77843-2128

Received 23 October 2002/Returned for modification 2 January 2003/Accepted 6 March 2003

Approximately 800 transcripts in *Saccharomyces cerevisiae* are cell cycle regulated. The oscillation of ~40% of these genes, including a prominent subclass involved in nutrient acquisition, is not understood. To address this problem, we focus on the mitosis-specific activation of the phosphate-responsive promoter, *PHO5*. We show that the unexpected mitotic induction of the *PHO5* acid phosphatase in rich medium requires the transcriptional activators Pho4 and Pho2, the cyclin-dependent kinase inhibitor Pho81, and the chromatin-associated enzymes Gcn5 and Snf2/Swi2. *PHO5* mitotic activation is repressed by addition of orthophosphate, which significantly increases cellular polyphosphate. Polyphosphate levels also fluctuate inversely with *PHO5* mRNA during the cell cycle, further substantiating an antagonistic link between this phosphate polymer and *PHO5* mitotic regulation. Moreover, deletion of *PHM3*, required for polyphosphate accumulation, leads to premature onset of *PHO5* expression, as well as an increased rate, magnitude, and duration of *PHO5* activation. Orthophosphate addition, however, represses mitotic *PHO5* expression in a *phm3*Δ strain. Thus, polyphosphate per se is not necessary to repress *PHO* transcription but, when present, replenishes cellular phosphate during nutrient depletion. These results demonstrate a dynamic mechanism of mitotic transcriptional regulation that operates mostly independently of factors that drive progression through the cell cycle.

Coordination of cell growth and division is essential to all living organisms and is innately tied to the cell division cycle. Periodic increases in certain transcripts at distinct cell cycle phases can meet specific, one-time requirements. For instance, nucleotide biosynthetic and histone genes are activated prior to and during S phase, respectively, to ensure adequate substrate concentrations for chromosomal duplication (9, 16). In addition, the sequential activation and proteolytic destruction of cyclins that partner with cyclin-dependent kinase (CDK) activities drives progression through the cell cycle (29). In contrast to this posttranslational mode of cell cycle control, it is clear that much cell cycle regulation occurs at the level of initiation of transcription by RNA polymerase II. In *Saccharomyces cerevisiae*, three major classes of transcriptional activators, MBF and SBF, Swi5/Ace2, and Mcm1-associated factors, predominantly regulate various gene clusters at the G_1/S transition; M and the M/G_1 boundary; and G_1, M, or M/G_1, respectively (42).

Spellman et al. (42) identified ca. 800 genes exhibiting cell cycle oscillation. While the regulation of ~500 of these genes can be ascribed to the three known classes of cell cycle transactivators, the mode of regulation of the rest is not understood. Many of these ~300 genes participate in nutrient acquisition, and their transcripts show peak expression in M or M/G_1. For instance, mitotic expression has been observed for genes involved in phosphate metabolism (28, 35) encoding low-affinity (*PHO89*) and high-affinity (*PHO84*) transporters of inorganic orthophosphate (P_i), as well as repressible acid phosphatases (rAPases; *PHO5*, *PHO11*, and *PHO12*) and constitutive APase (*PHO3*). Based on the timing of their expression, the mitotically induced rAPase genes are grouped with 34 other genes comprising the MCM cluster (42). However, there is no evidence for a direct or indirect role of Mcm1, or another known DNA binding cell cycle regulator, in their transcriptional activation. Moreover, as all the experiments of Spellman et al. (42) were conducted in rich medium that contained P_i, it is unclear why these *PHO* genes, which ordinarily are induced upon P_i deprivation, are activated during specific cell cycle phases. Thus, *PHO5*, *PHO11*, and *PHO12*, as well as other cell cycle-regulated *PHO* genes, fall into a large group of genes involved in maintaining nutritional homeostasis for which it is not understood how cell cycle periodicity is accomplished or why it is needed.

To date, studies of the mechanisms of yeast *PHO* gene activation have focused on regulatory events that occur in asynchronous cultures as a function of limiting P_i. By an as-yet-unknown mechanism, P_i limitation initiates a signal transduction cascade that activates Pho81, a CDK inhibitor. Pho81 inhibits the phosphorylation activity of the cyclin-CDK Pho80-Pho85 (39), leading to nuclear retention of the otherwise cytoplasmic helix-loop-helix factor Pho4, the primary PHO transactivator (22, 34). In the nucleus, Pho4, either by itself or as a heterodimer with Pho2, a nuclear homeodomain protein, activates >20 different genes in the *PHO* system (19, 33). These include several phosphate metabolism (*PHM*) genes, *PHM1* (*VTC2*), *PHM2* (*VTC3*), *PHM3* (*VTC4*), *PHM4* (*VTC1*), and *PHM5* (*PPN1*). Phm1 to -4 form a biochemical complex in vivo, the integrity of which is disrupted by *phm3* or *phm4* null mutations (6, 31). As polyphosphate (polyP), a linear polymer of up to hundreds of P_i residues linked by high-energy phosphoanhydride bonds, is not detectable in such strains, the Phm/Vtc complex is proposed to be a polyP synthetase (33). However, this complex is also needed for the proper morphology of

* Corresponding author. Mailing address: Department of Biochemistry and Biophysics, Texas A&M University, 2128 TAMU, College Station, TX 77843-2128. Phone: (979) 862-6677. Fax: (979) 845-9274. E-mail: kladde@tamu.edu.

vacuoles (31), where 99% of the total cellular polyP is stored (44).

PolyP is present in all organisms examined to date and, in *S. cerevisiae*, can reach concentrations as high as 120 mM in the vacuole, as much as 60% of the total phosphate content (23). It has been suggested that polyP functions as a phosphate reservoir, since its levels drop when cells need P_i, e.g., during log-phase growth or in P_i-limiting growth media (11, 41). It has also been suggested that polyP serves a cellular protective function in that it chelates cations, such as Ca^{2+}, in the vacuole (23). However, yeast strains deficient in polyP accumulation are not sensitive to high concentrations of calcium (33). Finally, polyP levels increase as yeast cultures approach stationary phase for reasons and by mechanisms that are not clear (40, 47). Thus, while conditions and enzymes involved in polyP synthesis and hydrolysis in eukaryotes have been identified, its metabolic, regulatory, and physiological function(s) remain obscure.

Relative to our understanding of the connection between nutrient sensing and the decision to execute Start (36), little is known about how nutrient levels influence regulation in other stages of the cell cycle. To gain insight into this problem, we have focused on elucidating both the molecular mechanisms and the physiological basis for M phase activation of *PHO5*. We report that the unexpected mitotic induction of *PHO5* in rich medium is under the control of Pho4, Pho2, and Pho81. Increasing the metabolic pools of polyP represses mitotic expression of *PHO5*. Conversely, elimination of polyP by deletion of *PHM3* leads to *PHO5* activation. Moreover, we demonstrate that polyP levels are influenced by progression of the cell cycle, declining prior to and being replenished after M phase. Our results suggest that polyP is a dynamic phosphate reserve, and they define a regulatory influence of polyP on *PHO* mitotic gene expression. Further, our studies demonstrate that Pho4/Pho2 mediates a novel, cell cycle stage-specific mode of regulation that is fine tuned in response to nutrient availability and operates mostly independently of activities that drive cell cycle progression. More generally, our findings suggest that nutrient deficiencies may underlie the transcriptional periodicity of a large class of nutrient transporters that are cell cycle regulated.

MATERIALS AND METHODS

Yeast strains and methods. All *S. cerevisiae* strains were constructed by standard genetic methods (37) from CCY694, *MAT***a**/*MAT*α *leu2Δ0*/*leu2Δ0 lys2Δ0*/*lys2Δ0 ura3Δ0*/*ura3Δ0 pho3*Δ::R/*pho3*Δ::R (S288C background) (2), where R is a *Zygosaccharomyces rouxii* recombinase site that remains after intramolecular recombination (21). The strains and their relevant (all are *MAT***a** *leu2Δ0 lys2Δ0 ura3Δ0 pho3*Δ::R) genotypes are DNY742 (wild type; *MAT***a** *bar1*Δ::R-*URA3*-R), THY868 (*MAT***a** *bar1*Δ::R-*URA3*-R *pho4*Δ::*kanMX4*), DNY989 (*MAT***a** *bar1*Δ::R-*URA3*-R *pho2*Δ::*kanMX4*), DNY925 (*MAT***a** *bar1*Δ::R-*URA3*-R *pho81*Δ::*kanMX4*), DNY986 (*MAT***a** *bar1*Δ::R-*URA3*-R *gcn5*Δ::*kanMX4*), DNY1309 (*MAT***a** *snf2*/*swi2*Δ::*kanMX4*), DNY1673 (*MAT***a** *bar1*Δ::R-*URA3*-R *phm3*Δ::*kanMX4*), DNY2464 (*MAT***a** *his3Δ1 phm1*Δ::*kanMX4*), DNY2465 (*MAT***a** *bar1*Δ::R-*URA3*-R *met15Δ0 phm2*Δ::*kanMX4*), and DNY2467 (*MAT***a** *bar1*Δ::R-*URA3*-R *his3Δ1 phm4*Δ::*kanMX4*).

Media and growth conditions. Cells were grown at 30°C on plates or in liquid cultures of complete synthetic medium– 2% glucose (Bio 101), yeast extract (Difco)– peptone (Difco)– 2% glucose (YPD), or YPD supplemented with 13.4 mM KH_2PO_4 (YPD + P_i) as appropriate. The defined P_i-free medium used in one step of the phosphate overplus experiments (see Fig. 5B), as well as for P_i starvation (see Fig. 2E and 9), contained 0.7 g of yeast nitrogen base without $(NH_4)_2SO_4$, phosphate, or amino acids (Bio 101), 2 g of glutamine, 20 g of glucose, and 3.9 g of MES (2-*N*-morpholino ethanesulfonic acid), pH 5.5, per liter.

All cultures, including overnight cultures, were maintained in early to mid-logarithmic phase growth. When P_i starvation was employed, the cells grew for only two to three additional generations after being washed and resuspended in P_i-free medium. Phosphate overplus experiments (see Fig. 5B) were performed as previously described (33); pregrowth in YPD or YPD-low P_i (YPD from which P_i was removed by precipitation) (15) followed by 2 h of P_i starvation in defined P_i-free medium and, finally, addition of KH_2PO_4 to 13.4 mM for 2 h. Note that while YPD is limiting for P_i (see Fig. 3 to 5), the designation YPD-low P_i indicates that the P_i concentration of the medium is decreased further but it is not P_i free. For measuring rAPase activities in asynchronous cultures (see Fig. 1D, 2D, 4A, and 5A), overnight cultures (10 ml) were grown and diluted the next day to an optical density at 600 nm (OD_{600}) of 0.03 in the appropriate fresh medium and incubated for another 6 h. For the P_i starvations (see Fig. 2E and 9), strains were plated on defined P_i-free medium with 13.4 mM KH_2PO_4 added back for 3 days. After overnight growth of starter cultures (10 ml) in the same medium, the cells were diluted in defined P_i-free medium at an OD_{600} of 0.2 and assayed at the appropriate times for rAPase activity and/or *PHO5* mRNA.

Cell cycle synchronizations, fluorescence-activated cell sorter analysis, and RNA-polyP isolation. Yeast cultures in early logarithmic growth in YPD were arrested at late G_1 and G_2/M by the addition of α-factor and nocodazole to final concentrations of 12 ng/ml and 17 μg/ml, respectively. After 2 h, the cells were released from cell cycle arrest by being filter washed three times and subsequently resuspended with YPD containing 0.1 mg of pronase E/ml (α-factor arrest) or YPD without pronase E (nocodazole arrest).

For flow cytometric analysis (FACSCalibur; Becton Dickinson), cells (1 ml) were removed every 15 min after release from cell cycle arrest and fixed overnight in 70% ethanol at 4°C. RNA was degraded by overnight incubation at 37°C in 50 mM sodium citrate, pH 7.1, containing 0.25 mg of RNase A/ml. The cells were then washed, and the DNA was stained by overnight incubation at 4°C in 50 mM sodium citrate, pH 7.1, containing 1 μM Sytox Green (Molecular Probes).

Total RNA isolation, which also recovers polyP, was performed as described by Cross and Tinkelenberg (7), except that the cells were resuspended in 350 μl of 1× LETS buffer (0.1 M LiCl, 10 mM EDTA, 10 mM Tris [pH 8.0], 0.5% [wt/vol] sodium dodecyl sulfate [SDS]) and 350 μl of acid phenol-chloroform (1:1) and lysed with glass beads by being vortexed at 4°C for 15 min. Following centrifugation of the mixture at 14,000 × *g* for 15 min, RNA and polyP were recovered from the aqueous phase by ethanol precipitation. The pellet consisting of RNA and polyP was resuspended in 0.1% SDS, quantified by absorbance at 260 nm, and stored at −80°C.

Northern hybridization and polyP analysis. For analysis of *PHO5* transcript levels, 10 μg of RNA was electrophoresed at 100 V for 3 h in 1% agarose gels buffered with 1× MOPS (3-*N*-morpholinopropanesulfonic acid) (20 mM MOPS [pH 7], 5 mM sodium acetate, 0.5 mM EDTA). RNA was blotted by 10× SSC (1.5 M NaCl, 0.15 M sodium citrate) to a positively charged nylon membrane. Membrane prehybridization and hybridization were performed in Church-Gilbert buffer (0.25 M Na_2HPO_4 [pH 7.4], 7% [wt/vol] SDS, 10 mg of fraction V bovine serum albumin/ml, 1 mM EDTA, and 0.5 mM sodium pyrophosphate). Hybridization probes, generated by PCR amplification using the oligonucleotide primers DNO425 (5′-TCTTTCCCTGGCGA-3′) and DNO426 (5′-GTCATCC AAGTAGGTTGTGT-3′) or DNO429 (5′-GCCAAGAAAGAGAGCTGC-3′) and DNO430 (5′-GAACTTAGAACCTGGTCTGTCC-3′) for *PHO5* and *TCM1*, respectively, were radiolabeled with [α-^{32}P]dCTP by random priming. mRNA levels were quantified by Storm 860 PhosphorImager analysis (Molecular Dynamics).

Gel analysis of polyP was performed by electrophoresis of 10 μg of RNA (containing copurifying polyP [see Fig. 5B] or treated with RNase A [see Fig. 7]) on native 6% polyacrylamide gels, followed by staining with toluidine blue O as described by Ogawa et al. (33). To quantify total levels of polyP, 10 μg of isolated RNA-polyP was treated with RNase A (after the removal of SDS by chloroform extraction, if necessary), and the polyP was ethanol precipitated and resuspended in 50 μl of distilled H_2O. Ten microliters of the purified polyP was mixed with 1 ml of toluidine blue solution (6 mg of toluidine blue O dye/liter, 40 mM acetic acid), and the metachromatic shift in the ratio of absorbance at 530 nm to that at 630 nm was measured (5). The A_{530}/A_{630} ratio of toluidine blue solution alone is a constant of 0.175, which was used as a blank. All samples were diluted to assure assay linearity, and polyP levels are expressed as $[(A_{530}/A_{630}) - 0.175]/\mu g$ of RNA. As expected, samples from a *phm3*Δ strain yield a value of zero.

Acid phosphatase activity assays. After the specified growth conditions were achieved, the cells were chilled to 4°C, washed twice, and resuspended in 0.1 M sodium acetate, pH 3.6, at 4°C. After preincubation (10 min) of 500 μl of cell

suspension at 30°C, the rAPase activity was assayed by addition of 500 μl of 20 mM *p*-nitrophenylphosphate (Roche) and incubation at 30°C for 10 min. Enzymatic activity was terminated by the addition of 250 μl of 1 M Na_2CO_3 and quantified by measuring the absorbance at 420 nm. Activities are reported in Miller units $\{(A_{420} \times 1{,}000)/(OD_{600} \times$ volume [in milliliters] of cells assayed $\times$ 10 min)$\}$.

RESULTS

Mitotic induction of *PHO5* requires the PHO activators Pho2, Pho4, and Pho81. Earlier genome-wide determinations of cell cycle-regulated transcripts suggested that *PHO5* and other *PHO* genes are induced during mitosis (42). However, significant cross hybridization of mRNA species can occur above 75% DNA sequence identity (17). Since *PHO5* and *PHO3* constitute a duplicated gene pair (87% identity over 1,404 bp), we reanalyzed the cell cycle expression profile of *PHO5* in a strain with the entire *PHO3* coding sequence deleted. Cultures in rich (YPD) medium were arrested at late G_1 with the mating pheromone α-factor and released synchronously by being washed with YPD. Northern analysis of RNA samples isolated at 15-min intervals demonstrates that *PHO5* mRNA levels oscillate during the cell cycle, with maximal expression occurring at 45 to 60 and 120 min after α-factor removal (Fig. 1A and B). Transcript from the ribosomal protein L3 locus, *TCM1*, remains constant throughout the cell cycle (4, 42) and serves as a loading control. Flow cytometric analysis confirmed that the cells synchronously traversed two cell cycles and that the points of maximal *PHO5* transcript accumulation coincide with M phase (Fig. 1C).

To examine whether the canonical PHO signal transduction pathway is involved in *PHO5* mitotic activation in YPD, we deleted three different positive regulators of the low-P_i induction pathway and assayed *PHO5* expression during synchronous growth in YPD. Deletions of *PHO4* and *PHO2*, encoding DNA site-specific transactivators of *PHO5*, abrogate mitotic induction of *PHO5* (Fig. 1A and B). A null allele of the CDK inhibitor *PHO81* eliminates ~95% of the mitotic expression. Since *PHO5* activation is completely dependent on Pho81 for inhibition of the Pho80-Pho85 cyclin-CDK (39), the residual level of expression in the *pho81*Δ strain is unexpected and suggests that a weaker, Pho81-independent activation mechanism also functions at *PHO5* during mitosis. We also determined the effects of the *pho2*, *pho4*, and *pho81* null mutations on rAPase activity in asynchronous cultures, which can often be used to observe cell cycle-dependent events (20). Approximately 60 to 110 U of rAPase activity are detected in asynchronous YPD cultures of wild-type strains (Fig. 1D and 2D; also see Fig. 4A and 5). Enzyme activity is reduced by >99% in *pho4*Δ and *pho2*Δ strains. Despite the residual level of mitotic *PHO5* mRNA, rAPase activity is also eliminated in the *pho81*Δ strain. We conclude that most of the measurable rAPase activity in asynchronous YPD cultures of strain DNY742 (*pho3*Δ) can be attributed to expression of *PHO5*, and presumably that of the minor rAPases *PHO11* and *PHO12*, in M phase (4, 42). Further, mitotic induction of *PHO5* is strongly dependent on the positive PHO effectors *PHO4*, *PHO2*, and *PHO81*.

Mitotic activation of *PHO5* requires the chromatin remodelers Gcn5 and SNF/SWI. Next, we investigated the requirements, in mitotic activation of *PHO5*, for chromatin-remodeling enzymes, including Gcn5, the catalytic subunit of several histone H3 acetyltransferase complexes (3, 12), and the Snf2/Swi2 ATPase subunit of the SNF/SWI chromatin-remodeling complex (27). Since *gcn5*Δ cells could not be arrested with α-factor, presumably because Gcn5 is required for expression of the CDK inhibitor *FAR1* (18), we synchronized cells in G_2/M with nocodazole, an inhibitor of microtubule polymerization. After release from G_2/M, wild-type cultures progressed through three cell cycles and showed maximal *PHO5* induction at 15, 105, and 150 min (Fig. 2A and B), each peak corresponding to M phase (Fig. 2C). In contrast, no induction was observed in the *snf2*/*swi2*Δ and *gcn5*Δ strains, indicating that mitotic induction of *PHO5* is highly dependent on these transcriptional coactivators. Greater than 90% of the rAPase activity of asynchronous cultures is eliminated in each null strain, demonstrating that synchrony is not required to observe the requirement for SNF/SWI and Gcn5 (Fig. 2D). We con-

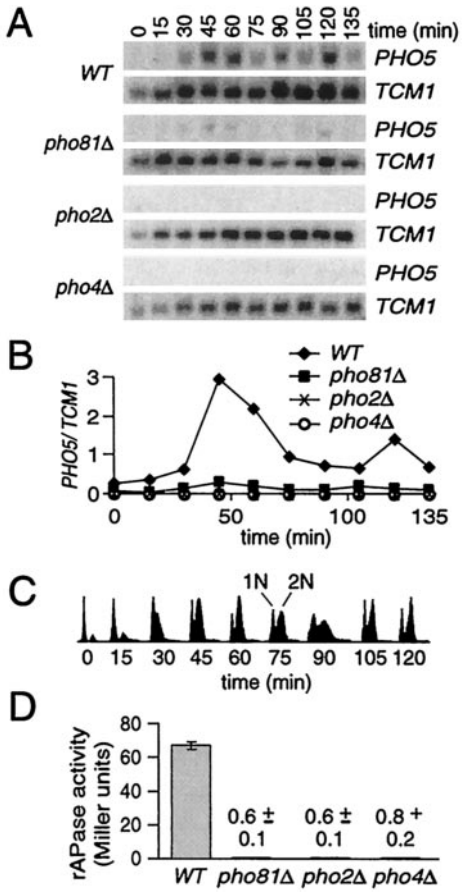

FIG. 1. Mitotic induction of *PHO5* requires *PHO2*, *PHO4*, and *PHO81*. (A) Northern analysis of wild-type (*WT*), *pho81*Δ, *pho2*Δ, and *pho4*Δ cultures at various times following release from synchronization with α-factor. The wild-type strain was analyzed in parallel with each null strain as a positive control. (B) Transcript levels of *PHO5* (normalized to *TCM1*) from panel A. (C) Flow cytometric analysis of Sytox Green-stained cells. The *x* and *y* axes indicate the fluorescence intensity and numbers of cells analyzed (which was identical in all panels), respectively. 1N and 2N refer to haploid and diploid DNA contents, respectively. (D) Total rAPase activities of asynchronous YPD cultures. The means ± 1 standard deviation from three independent experiments are shown.

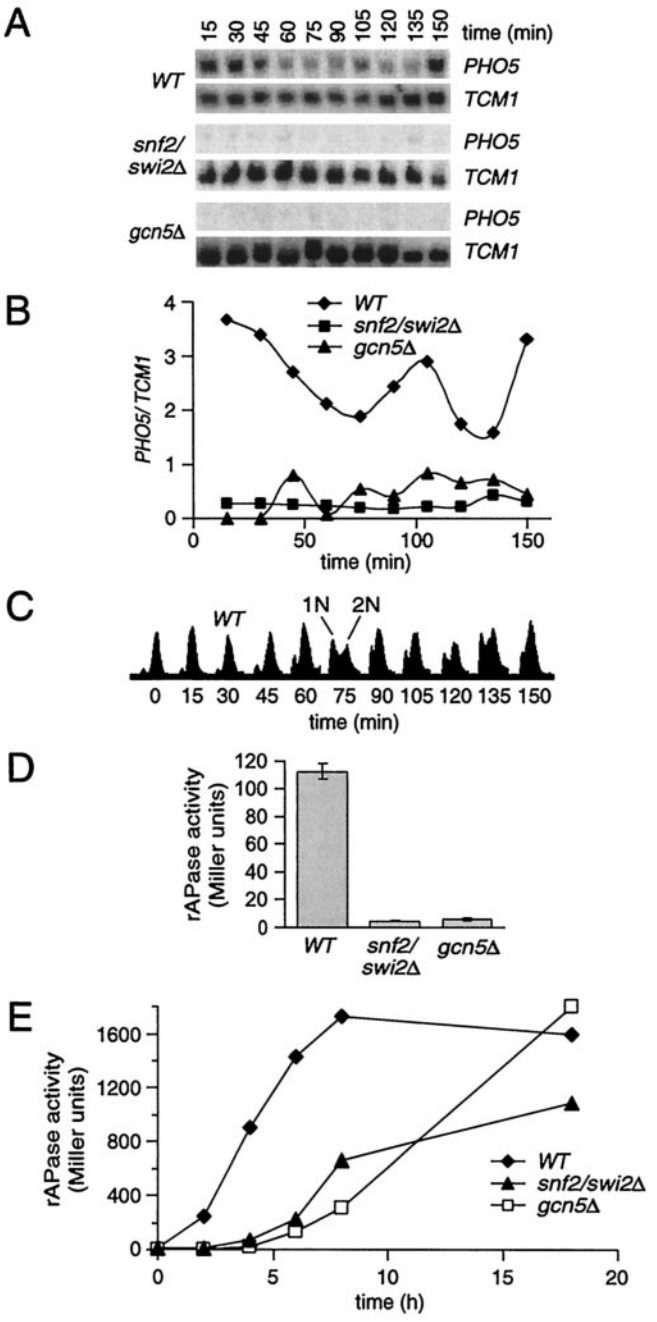

FIG. 2. *PHO5* activation is SNF/SWI and Gcn5 dependent. (A) Northern analysis of synchronous cultures of wild-type (*WT*), *snf2/swi2*Δ, and *gcn5*Δ strains released from nocodazole arrest in YPD medium. (B) Normalized *PHO5* transcript levels from panel A. (C) Flow cytometric analysis of wild-type cells in panel A. (D) Total rAPase activities of asynchronous YPD cultures ($n = 3$; mean ± 1 standard deviation). (E) Time course of *PHO5* activation. Asynchronous cultures grown on defined P_i-free medium with 13.4 mM P_i added back were starved for P_i and assayed for total rAPase activity at the indicated times.

clude that the previously reported Gcn5- (18) and Snf2/Swi2-dependent (43) transcription of *PHO5* in asynchronous YPD cultures is explained by the pronounced need for these enzymes in *PHO5* mitotic expression.

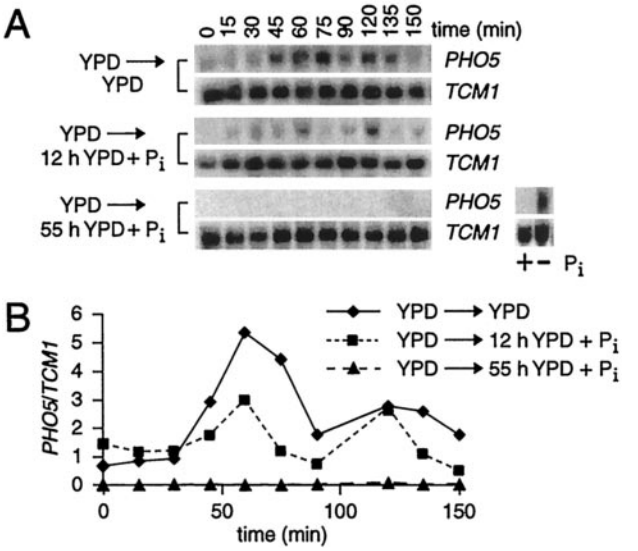

FIG. 3. *PHO5* mitotic activation is repressed by addition of orthophosphate (P_i). (A) Northern analysis of α-factor-synchronized cultures. Single colonies from a YPD plate were inoculated into YPD overnight cultures and then diluted in YPD or YPD + P_i (13.4 mM) for 12 or 55 h (as indicated on the left) prior to α-factor arrest. Cells grown for 6 h in defined P_i-free medium with (+) or without (−) P_i were included as a positive control in the Northern analysis of the samples grown for 55 h in YPD + P_i. (B) Normalized *PHO5* transcript levels from panel A.

Previous studies using asynchronous cell populations demonstrated that SNF/SWI and Gcn5 are not required for activation of *PHO5* following overnight starvation for P_i (10, 14). More recently, it has been shown that deletion of *GCN5* decreases *PHO5* activation at early times after P_i starvation, but not 8 h postactivation (1). Figure 2E demonstrates that asynchronous cultures of *gcn5*Δ and *snf2/swi2*Δ strains both exhibit a decreased initial rate of *PHO5* transactivation following transfer to P_i-free medium. Thus, we have defined novel requirements for transcriptional coactivators at *PHO5*, including *PHO5* among other genes for which activation in M phase is strongly Gcn5 and SNF/SWI dependent (24). Our data also confirm a role for Gcn5 in the rate of *PHO5* activation and extend this observation to the SNF/SWI complex.

Mitotic activation of *PHO5* occurs under conditions of limiting P_i. Activation of *PHO5* by Pho4 in asynchronous cultures is dependent on P_i deprivation and, ordinarily, is rapidly repressed by the addition of exogenous P_i (38). Since increased *PHO5* transcription during mitosis is Pho4 dependent (Fig. 1), we tested if this cell cycle-specific activation in YPD is responsive to P_i levels. Surprisingly, despite 12 h of growth in YPD + P_i prior to α-factor arrest and release, mitotic activation of *PHO5* is still apparent (Fig. 3). However, when the incubation in YPD + P_i is extended to 55 h before α-factor synchronization, *PHO5* transcript is not detectable. This result indicates that exogenous P_i attenuates mitotic induction of *PHO5* in a time-dependent manner.

Next, we further investigated the time dependence of repression of mitotic *PHO5* induction. Relative to cells growing continuously on YPD, rAPase activity decreased by 50% when the cultures were shifted from YPD to YPD + P_i (Fig. 4A, com-

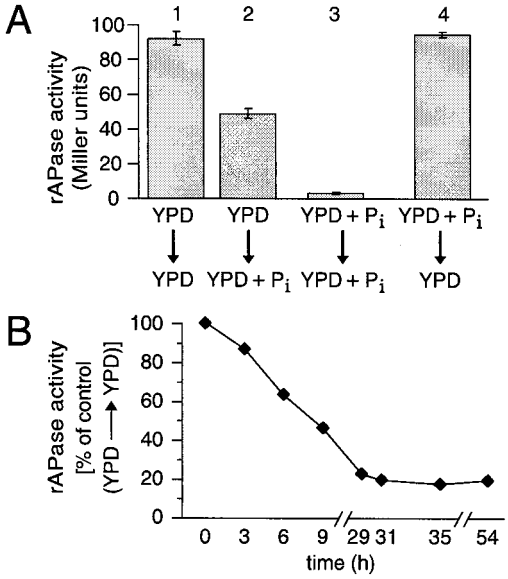

FIG. 4. Repression of *PHO5* mitotic expression by added P_i is time dependent. (A) Total rAPase activities of asynchronous cultures. Cultures were grown overnight in either YPD (bars 1 and 2) or YPD + P_i (bars 3 and 4) and then washed and resuspended in YPD (bars 1 and 4) or YPD + P_i (bars 2 and 3) for an additional 6 h, as indicated (n = 3; mean ± 1 standard deviation). (B) Time course of decrease in total rAPase activity following addition of P_i. Cells were plated and pregrown on YPD and transferred to YPD (control) or YPD + P_i. The percentage of activity of the control (growth in parallel in YPD) is plotted as a function of time.

pare bars 1 and 2). Full repression of *PHO5* required longer incubation in YPD + P_i (compare bars 1 and 3). In the opposite experiment, pregrowth on YPD + P_i and shift to YPD, full derepression is restored (compare bars 1 and 4). This result suggests that repression of mitotic expression takes longer than its induction. The time required to achieve full repression of *PHO5* was assessed by pregrowth of cells in YPD followed by transfer to YPD + P_i. As in Fig. 4A, rAPase activity was reduced to ~60% of that of the control YPD culture at 6 h (Fig. 4B). Maximal *PHO5* repression was achieved after ~29 h and remained at this level for the rest of the time course. The time required to reach full repression is not likely due to rAPase stability, since the half-life of rAPase activity is 2 to 2.5 h, as determined by the phosphate overplus procedure (P_i starvation followed by P_i addition; see Materials and Methods and data not shown). The remaining activity may be due to basal levels of *PHO5* expression and that of the more minor rAPases, *PHO11* and *PHO12*, which vary somewhat between experiments. These findings demonstrate that YPD can be limiting for P_i. The lag in full repression may be due to active growth in YPD that leads to rapid metabolism of a PHO-repressive signal.

PolyP reserves increase, but are not essential for, repression of *PHO5*. PolyP is the most prevalent form of phosphate in yeast, and it is believed to serve as a phosphate reservoir (11, 41, 44). Such a phosphate reservoir might sustain intracellular P_i levels more effectively during P_i deprivation and hence repress M phase expression of *PHO5*. To test this hypothesis, we asked if strains singly null for four *PHM* genes had increased levels of total rAPase activity. Strains with *PHM3* and *PHM4* deleted are severely deficient in the Phm/Vtc complex and thus lack detectable polyP, but they do not exhibit growth defects. The phenotypic defects of *phm1*Δ and *phm2*Δ strains are much less pronounced (31, 33). In the experiment shown in Fig. 5A, each strain was grown in YPD and then diluted in YPD or YPD + P_i for 6 h. Relative to wild-type cells, rAPase activity during continuous growth in YPD increases 2- to 2.5-fold in *phm3*Δ or *phm4*Δ strains and only modestly in *phm1*Δ or *phm2*Δ cells (Fig. 5A). Thus, the magnitude of *PHO5* derepression under P_i-limiting conditions (YPD) correlates well with the severity of the polyP accumulation defect and extent of disruption of Phm/Vtc complex integrity: *phm1*Δ ≈ *phm2*Δ < *phm3*Δ ≈ *phm4*Δ (31, 33). Interestingly, incubation in YPD + P_i for 6 h reverses the *PHO5* derepression, and lower levels of expression are established in the absence of Phm3 and Phm4.

To explore the relationship between *PHO5* mitotic activation and polyP levels further, we tested if high-P_i conditions increase cellular polyP and, if so, its effects on total rAPase activity. Consistent with our finding that YPD is limiting for P_i (Fig. 3 to 5A), a wild-type (*PHM3*) strain grown in YPD has low but significant levels of polyP (Fig. 5B, lane 1). The isogenic *phm3*Δ strain has no detectable polyP (33) (Fig. 5B, compare lanes 1 and 3). In this experiment, rAPase activity is increased fourfold in the *phm3*Δ strain relative to the wild-type strain, again demonstrating that loss of polyP leads to increased *PHO5* activation in YPD. When wild-type (*PHM3*) cells are grown in high-P_i medium (YPD + P_i), polyP amounts increase 5-fold (Fig. 5B, compare lanes 1 and 4), which is accompanied by a 10-fold reduction in rAPase activity and undetectable *PHO5* transcript levels in M phase (Fig. 3). During growth in complete synthetic medium (7.3 mM P_i), wild-type strains accumulate levels of polyP [0.07 (A_{530}/A_{630})/μg of RNA] and rAPase (13 U) activities similar to those in YPD + P_i (13.4 mM). As expected, the *phm3*Δ strain had no detectable polyP in YPD + P_i (33) but, as in Fig. 5A, had repressed levels of rAPase activity (Fig. 5B, lane 2). This indicates that polyP is not required to repress *PHO5* when P_i is plentiful. We conclude that, under conditions of limiting P_i, accumulated polyP acts as a cellular phosphate reserve that can contribute to the repression of *PHO5* expression. However, as *PHO5* is completely repressed by excess P_i in strains that are unable to accumulate polyP, the polymer is not necessary for *PHO5* promoter inactivation.

When *S. cerevisiae* encounters a period of P_i starvation followed by a high-P_i environment, a phenomenon called "overplus" or "overcompensation" occurs in which large amounts of polyP accumulate (23). This method was previously used to evaluate the role of *PHM* genes in polyP synthesis (33). In parallel with the samples in Fig. 5B, lanes 1 to 4, wild-type cells subjected to the overplus procedure (see Materials and Methods) accumulate 60-fold more polyP than during continuous growth in YPD (Fig. 5B, compare lanes 5 and 1). Interestingly, overplus polyP levels surpass those of cultures grown continuously in YPD + P_i (compare lanes 4 and 5). The highest level of polyP is observed upon growth in YPD-low P_i before the addition of P_i (compare lanes 6 and lanes 1 to 5). Therefore, the amount of polyP that accumulates during the overplus procedure is proportional to the severity of prior P_i starvation,

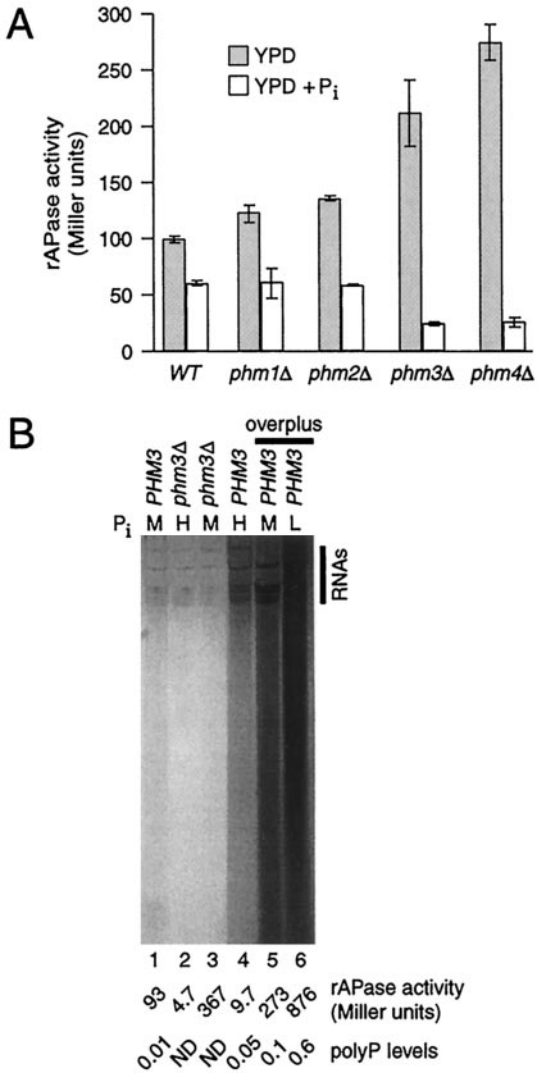

FIG. 5. Loss of polyP leads to derepression of *PHO5*. (A) Total rAPase activities of wild-type (*WT*), *phm1*Δ, *phm2*Δ, *phm3*Δ, and *phm4*Δ strains. Cells were grown in YPD and diluted in YPD or YPD + P_i medium for 6 h prior to assay of rAPase activity ($n = 3$; mean ± 1 standard deviation). The severity of loss of polyP accumulation increases from left to right and parallels the extent of disruption of the Phm/Vtc complex, with *phm3*Δ and *phm4*Δ strains having no detectable polyP or Phm/Vtc complex (31, 33). (B) Analysis of polyP levels. Wild-type (*PHM3*) or *phm3*Δ strains were grown for 2 days on plates and then for 24 h in liquid YPD-low P_i, YPD, or YPD + P_i medium containing a low (L; lane 6), moderate (M; lanes 1, 3, and 5), or high (H; lanes 2 and 4) concentration of P_i, respectively. For lanes 1 to 4, after the 24-h incubation period, internal aliquots of each culture were assayed for rAPase activity and polyP levels by the metachromatic absorbance shift method (as indicated at the bottom; ND, nondetectable). The overplus samples (lanes 5 to 6) received additional treatments of P_i starvation followed by P_i addition (see Materials and Methods) before rAPase and polyP levels were determined. PolyP was also visualized in the gel after electrophoresis of equal amounts (10 μg) of total RNA and staining with toluidine blue O dye, a basic dye that binds polyanions. RNA species at the top of the gel are indicated on the right.

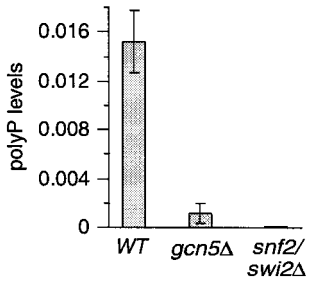

FIG. 6. SNF/SWI and Gcn5 are required for polyP accumulation. Steady-state levels of polyP from wild-type (*WT*), *gcn5*Δ, and *snf2/swi2*Δ strains were measured ($n = 3$; mean ± 1 standard deviation) by the metachromatic shift method after asynchronous growth in YPD (the same conditions used for rAPase activity measurements in Fig. 2D).

consistent with increased transcription of *PHM* and/or other genes that may play direct or indirect roles in polyP biosynthesis (19, 33). In contrast, as relatively high levels of polyP are synthesized in wild-type cells when excess P_i is present, polyP synthesis does not require a preceding period of P_i starvation.

Accumulation of polyP under limiting P_i conditions requires SNF/SWI and Gcn5. The levels of polyP and *PHO5* expression are inversely correlated (Fig. 5B, lanes 1 and 4 or 3 and 4). Thus, the loss of mitotic *PHO5* activation in *snf/swi* and *gcn5* mutants (Fig. 2) might be due to a pleiotropic hyperaccumulation of polyP. We determined, however, that polyP levels were decreased >10-fold and near the detection limit in *gcn5*Δ and *snf2/swi2*Δ strains, respectively, during continuous growth in YPD (Fig. 6). This result suggests that SNF/SWI and Gcn5 are needed for M phase activation of *PHM* genes, as well as *PHO5*, when P_i is limited.

PolyP levels fluctuate during the cell cycle. Because *PHO5* expression is inversely related to polyP reserves (Fig. 5), we investigated if mitotic activation of *PHO5* is correlated with a decrease in polyP levels before M phase in α-factor-synchronized cultures (Fig. 7). Maximal levels of polyP are observed at G_1 (0 to 15 min) and reach a minimum when cells are well into S phase, 45 to 60 min after α-factor removal. The 6- to 10-fold increase in polyP levels compared to Fig. 5B and 6 is reproducibly observed following synchronization. Nevertheless, a four- to fivefold drop in polyP levels precedes peak accumulation of *PHO5* mRNA in mitosis, which occurs at 75 min. PolyP amounts remain at the minimum through 105 min and then increase fivefold at 120 min. Presumably, this is because enhanced mitotic expression of *PHO5* (Fig. 7B), other rAPase genes, and *PHO84*, the high-affinity P_i transporter, lead to increased scavenging of P_i and hence polyP synthesis. These data indicate that, in P_i-limiting medium (e.g., YPD), polyP levels fluctuate with the cell cycle. Importantly, this result also suggests that the physiological basis for mitotic cycling of *PHO5* is due to significant, but not complete, depletion of polyP reserves prior to M phase.

Loss of polyP increases the rate, magnitude, and duration of *PHO5* activation. We also assessed the effects of the absence of polyP deficiency on *PHO5* activation during synchronous cell cycle progression. Following α-factor synchronization and release in YPD medium, induction of *PHO5* in the *phm3*Δ strain, which lacks detectable polyP (33), increases dramatically in

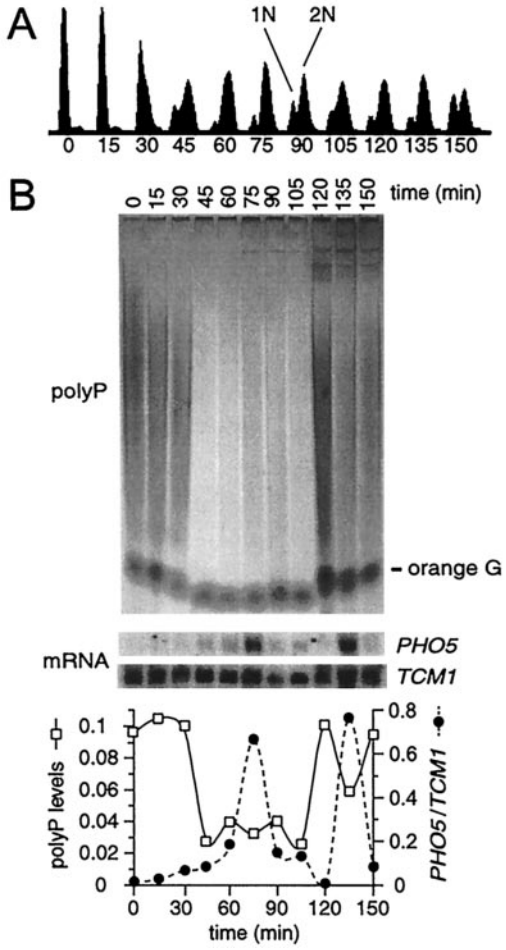

FIG. 7. PolyP levels fluctuate during the cell cycle. (A) Flow cytometric analysis of α-factor-synchronized cultures. (B) Analysis of polyP and mRNA levels. Total RNA and polyP were isolated at 15-min intervals following release from α-factor arrest. PolyP was analyzed as for Fig. 5B, except that the samples were treated with RNase A prior to electrophoresis (polyP gel) and metachromatic shift quantification of polyP levels of an internal fraction (graph at bottom). Northern analysis of *PHO5* and *TCM1* mRNA levels of internal aliquots of RNA-polyP not treated with RNase A (middle) are plotted versus time and compared to polyP levels at the bottom.

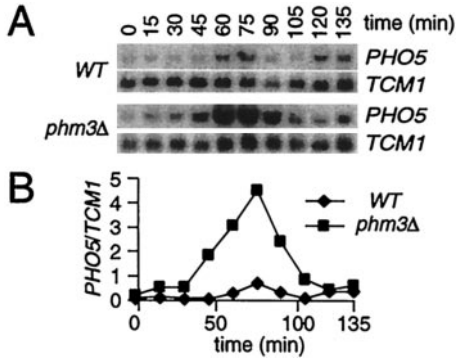

FIG. 8. Mitotic activation of *PHO5* is increased in *phm3*Δ strains. (A) Northern analysis of α-factor-synchronized cultures of wild-type (*WT*) and *phm3*Δ cells. (B) Normalized *PHO5* transcript levels from panel A.

comparison to that in wild-type cells (Fig. 8). Furthermore, *PHO5* mRNA was evident earlier in the *phm3*Δ strain, indicating that the null cells lose the repressive signal inactivating *PHO5* transcription before their wild-type counterparts. Flow cytometric analysis demonstrated that the length and timing of each cell cycle phase in the *phm3* strain was indistinguishable from those in the wild type (data not shown), consistent with its wild-type growth phenotype (6). Therefore, the absence of Phm3 causes increased levels of *PHO5* transcription that are not due to a higher proportion of cells in M phase.

Strains lacking the Phm/Vtc complex are defective in sustaining transport of P_i that is added during the overplus procedure (33), making it possible that *PHO5* would be derepressed (26). However, a low level of *PHO5* transcript that precedes and follows the mitotic peak (Fig. 8) strongly suggests that *PHO5* transcription is not constitutively derepressed in *phm* strains. Alternatively, it was hypothesized (33) that compromised P_i transport could indirectly result from the inability to synthesize polyP; the failure to divert added P_i to vacuoles leads to increased cytosolic P_i concentrations that signal degradation of Pho84, the high-affinity P_i transporter (48). Nevertheless, employing the overplus treatment with asynchronous wild-type and *phm3*Δ cultures, an identical precipitous drop in *PHO5* transcript levels occurs from 20 to 30 min after P_i addition (data not shown). We conclude that the initial 5-min period of P_i transport observed in *phm3*Δ cells during the phosphate overplus (33) is sufficient to signal *PHO5* repression.

The rapid onset of accumulation of *PHO5* transcript in the *phm3*Δ strain (Fig. 8), even prior to G_2/M, where all cells have achieved a 2N DNA content, suggests an increased rate of *PHO5* activation in the absence of polyP reserves. To evaluate this possibility, we tested how polyP stores influence the initial rate of *PHO5* mRNA accumulation in asynchronous cultures in response to P_i starvation (Fig. 9). Wild-type and *phm3*Δ strains were first grown in defined P_i-free medium with 13.4 mM P_i added back so that substantial cellular polyP would accumulate. Subsequently, P_i was removed by washing, both cultures were shifted to P_i-free medium, and the levels of *PHO5* mRNA, as well as rAPase activity, were monitored over time. *PHO5* transcript accumulates linearly in both the wild-type ($R^2 = 0.96$) and *phm3*Δ ($R^2 = 0.99$) strains for 150 and 60 min, respectively. Strikingly, the initial, rapid response to P_i starvation occurs 60 min earlier and at a threefold-higher rate in the *phm3*Δ strain. Moreover, *PHO5* transcript levels in the *phm3*Δ strain are significantly higher (120-fold more at 60 min) at every time point up to and including 4 h, achieve maximum 2 h earlier, and are maintained at this higher level longer than in wild-type cells. Subsequently, *PHO5* mRNA levels plateau and then, interestingly, decline to similar levels in both cultures around 6 h after P_i starvation. As expected, the levels of internally assayed rAPase activity lag behind and qualitatively support these observations (Fig. 9A). The absence of a decrease in rAPase activity at the later time points likely reflects the increased stability of the protein relative to *PHO5*, *PHO11*, and *PHO12* transcripts (46). We conclude that the initial rates of accumulation of *PHO5* transcript and rAPase activity, and presumably the rates of transcriptional initiation, are enhanced in

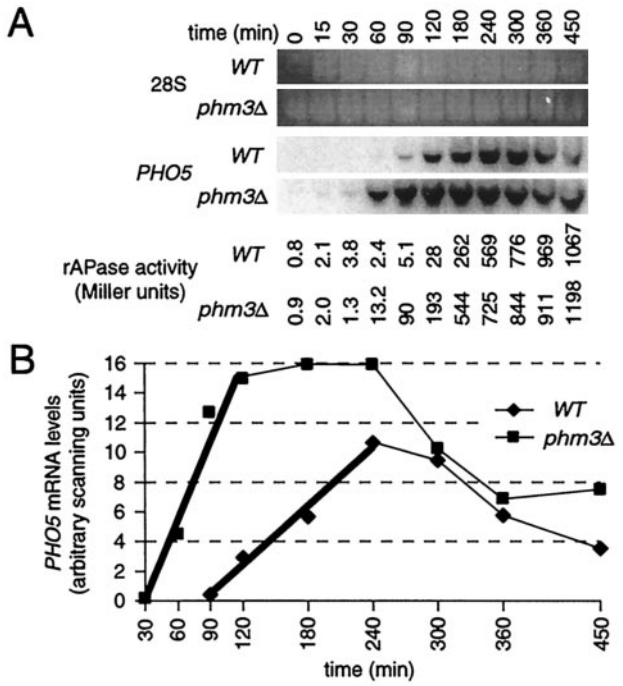

FIG. 9. Deletion of *PHM3* increases the rate of *PHO5* activation. (A) Northern analysis of RNA isolated during a time course of *PHO5* activation. Wild-type (*WT*) and *phm3*Δ strains grown on defined P_i-free medium with 13.4 mM P_i added back (to build up stores of polyP in the wild-type strain) were then starved for P_i by being washed and resuspended in P_i-free medium, and RNA was isolated at the indicated times. The total rAPase activities obtained from an internal aliquot of each culture are indicated below each lane. (B) Absolute *PHO5* transcript levels from panel A. The thick trend line indicates the initial, linear period of transcript accumulation.

cells lacking polyP. Further, the repressive influence of polyP reserves on *PHO5* transcription was observed in a defined medium, which complements our results obtained using YPD medium.

DISCUSSION

We have investigated the molecular mechanisms and physiological basis for activation of *PHO* promoters, which are in a prominent class of mitotically induced genes with nutritional roles (42). In contrast to previous findings using P_i-starved, asynchronous cultures, we find that *PHO5* activation in M phase in synchronized cultures grown in rich medium is strongly dependent on the SNF/SWI complex, an ATP-dependent chromatin remodeler, and the histone acetyltransferase Gcn5 (Fig. 2). Additionally, our work shows that M phase induction of *PHO5* requires the transactivators Pho2 and Pho4, as well as the CDK inhibitor Pho81, suggesting that *PHO5* mitotic induction occurs through the PHO signal transduction pathway (Fig. 1). In accord with this, addition of exogenous P_i suppresses mitotic activation of *PHO5* (Fig. 3) and increases polyP levels, which are inversely correlated with *PHO5* expression in wild-type cells (Fig. 5B). Further, in synchronized cultures, polyP amounts decrease between G_1 and M phases, demonstrating that metabolic pools of polyP fluctuate during the cell cycle (Fig. 7). Beyond these correlations, we show that strains with undetectable levels of polyP (*phm3*Δ) exhibit a dramatically enhanced PHO response in both synchronous and asynchronous cultures (Fig. 8 and 9). These results establish that polyP causally represses *PHO5* expression. Moreover, the physiological stimulus for activation of *PHO5* in M phase is P_i depletion that ensues after reduction of vacuolar polyP reserves. Thus, our results expand the role of the *PHO* signaling system to include coordination of the mitotic activation with P_i availability during cell cycle progression. Our data also highlight a novel function for polyP as a negative regulator of *PHO* activation in mitosis.

Our findings support the model that a central, physiological role of polyP is that of a phosphate reservoir (11, 41). Under conditions of limiting P_i, inasmuch as degradation of polyP increases intracellular P_i pools, the polymer antagonizes *PHO5* activation. It is likely that our findings apply generally to other *PHO* (and *PHM*) genes, since the rate of *PHO84* transcript accumulation is also enhanced upon P_i starvation in a *phm3*Δ strain (D. W. Neef and M. P. Kladde, unpublished data). It must be emphasized that Phm/Vtc complex activity, and hence polyP, is not required to maintain (Fig. 9, zero point) or establish (Fig. 5) repression of *PHO5* when P_i is abundant. Further, a lack of detectable polyP does not impair the ability to repress *PHO5* transcription before and after the mitotic peak in synchronized populations (Fig. 8). Thus, polyP is a modulator rather than an essential cell cycle regulator of *PHO* expression, replenishing intracellular levels of P_i when metabolic demand for it is high.

The inability to make polyP in the absence of the Phm/Vtc complex allowed us to address the interplay between polyP and *PHO5* regulation during M phase. Extensive P_i starvation leads to G_1 arrest (30), primarily due to controls that operate at Start (36). Although the mechanisms are unclear, it is widely accepted that these controls involve attaining sufficient cell size and nutrient acquisition for cell division. In view of this, while cells have already gauged sufficient phosphate resources to execute Start, why do they rapidly mobilize their polyP reserves with synchronous progression through S phase (Fig. 7)? It is possible that polyP reserves are directly sensed as a P_i source prior to Start. However, if this were the case, constitutive activation of *PHO5* outside of M phase would be expected in the absence of polyP (*phm3*Δ cells), which is not observed (Fig. 8). Instead, since *phm3*Δ cells lack reserve P_i afforded by polyP, they exaggerate mitotic induction of *PHO* genes (Fig. 8). Thus, while the cell division commitment decision is made at G_1, our data suggest that the sensing of and response to nutrient imbalances is not restricted to G_1 (45). This view is supported further by the fact that *PHO5* is strongly activated by P_i starvation during sustained mitotic arrest (Neef and Kladde, unpublished). Since the cells could not anticipate the post-Start starvation, we conclude that they are able to sense P_i at cell cycle stages other than G_1.

We propose the following model for *PHO5* mitotic activation under conditions of limiting P_i (e.g., YPD). A yeast cell maintains cytosolic P_i at levels sufficient to satisfy metabolic needs and stores any excess as polyP. Upon reaching critical size and nutrient status, the cell will initiate Start and probably decrease cytosolic P_i rapidly while synthesizing nucleotides for DNA replication and transcription, as well as phospholipids for the enlarging bud. PolyP reduction also correlates with

marked increases in sugar phosphates during synchronous entry into S phase (11, 32). As the intracellular P_i concentration declines and is unable to be replenished by preferred extracellular P_i (11), it may first be more expedient to degrade polyP to P_i, presumably via endopolyPases (Ppn1) and exopolyPases (25, 40). Subsequently, when polyP reserves and hence cytosolic P_i fall critically low, transcription of the *PHO* and *PHM* genes is activated. During M phase, and possibly into G_1, rAPase synthesis leads to hydrolysis of phosphoesters in the medium, which supplies P_i for import via the high-affinity transporter Pho84, which is also expressed in mitosis (42). Increased cytosolic P_i (or some anabolite of P_i) leads to attenuation of the *PHO* mitotic induction. After metabolic growth requirements are met, excess P_i is assimilated into polyP, thus reconciling the seeming paradox that cells synthesize polyP in response to P_i deprivation.

The primary reason for *PHO* mitotic expression may be to sequester as much P_i as is feasible as vacuolar polyP. This view is supported by the fact that *pho4*Δ cells exhibit a wild-type growth rate in YPD, despite the absence of detectable polyP (33) (Fig. 5B) and inability to activate *PHO* genes in mitosis (Fig. 1). Hence, the amount of P_i (or phosphate esters) and basal levels of *PHO* gene expression are adequate for *pho4*Δ cells to meet their P_i growth requirements. Therefore, mitotic PHO activation may simply confer an adaptive advantage through hoarding P_i as polyP or significant conservation of transcriptional resources, antagonizing excessive activation of *PHO5* (Fig. 8 and 9) and ~20 additional *PHO*, *PHM*/*VTC*, and other genes (19, 33).

We find that activation of *PHO5* during mitosis in YPD and the initial period of P_i starvation are strongly dependent on SNF/SWI and Gcn5 (Fig. 2). In contrast, activation of *PHO5* in asynchronous cultures extensively starved for P_i is refractory to the loss of both chromatin-remodeling activities (10, 13). This apparent discrepancy is potentially explained by a global requirement for Gcn5 and SNF/SWI in mitotic gene expression (24). The relatively short period (~15 to 30 min) of mitotic activation may also contribute to the pronounced Gcn5 and SNF/SWI dependence, since these coactivators are needed for wild-type rates of *PHO5* activation (1) (Fig. 2E). Because *snf*/*swi* and *gcn5* mutants have very low levels of polyP (Fig. 6), it is unlikely that they exhibit lower rates of *PHO5* activation due to impaired growth and hence slower depletion of cellular P_i. Moreover, the rates of transactivation of double *snf*/*swi phm3* and *gcn5 phm3* mutants with undetectable polyP are also lower than those of *phm3* cells (data not shown).

PHO5 transcription is also Gcn5 and SNF/SWI dependent in asynchronous cultures grown in YPD (18, 43) but does not require SNF/SWI in synthetic minimal medium (43). We propose that this medium-specific difference for SNF/SWI can now be explained in terms of polyP. Mitotic expression in YPD is significant due to its low levels of P_i and hence vacuolar polyP. In contrast, the high P_i concentration (7.3 mM) of minimal medium leads to substantial increases in polyP that repress M phase expression (Fig. 5).

The antagonism between polyP/P_i levels and the magnitude of PHO activation suggests that nutrient sensing may underlie the transcriptional periodicity of other cell cycle-regulated genes. In particular, transcripts for genes involved in the transport of a variety of nutrients in addition to P_i, including carbohydrates, heavy metals, ions, and amino acids, fluctuate during the cell cycle (42). Genes involved in glycogen (*GSY1*) and fatty acid (*FAA1* and *FAS1*) synthesis are also cell cycle regulated in rich medium. Depending on the particular sensing system, the presence or absence of nutrients may lead to periodic increases or decreases in cell cycle transcription. Alternatively, the low levels of P_i in YPD may contribute indirectly to the periodic expression of some genes. For example, mitotic induction of the plasma membrane ATPase, *PMA1*, may generate the proton gradient that is requisite for Pho84-mediated symport of P_i (and many other nutrients). Finally, since polyP chelates cations (8), it is plausible that their uptake is coordinated with polyP synthesis. It remains to be seen if the loss of polyP affects the transcription of any of these additional cell cycle-regulated genes.

ACKNOWLEDGMENTS

We thank Christopher Carvin for strains and Mary Bryk, Michael Polymenis, and members of our laboratory for critical reading of the manuscript.

This work was supported in part by a grant from the Texas Higher Education Coordinating Board.

REFERENCES

1. **Barbaric, S., J. Walker, A. Schmid, J. Q. Svejstrup, and W. Hörz.** 2001. Increasing the rate of chromatin remodeling and gene activation—a novel role for the histone acetyltransferase Gcn5. EMBO J. **20:**4944–4951.
2. **Brachmann, C. B., A. Davies, G. J. Cost, E. Caputo, J. Li, P. Hieter, and J. D. Boeke.** 1998. Designer deletion strains derived from *Saccharomyces cerevisiae* S288C: a useful set of strains and plasmids for PCR-mediated gene disruption and other applications. Yeast **14:**115–132.
3. **Brownell, J. E., J. X. Zhou, T. Ranalli, R. Kobayashi, D. G. Edmondson, S. Y. Roth, and C. D. Allis.** 1996. *Tetrahymena* histone acetyltransferase A: a homolog to yeast Gcn5p linking histone acetylation to gene activation. Cell **84:**843–851.
4. **Cho, R. J., M. J. Campbell, E. A. Winzeler, L. Steinmetz, A. Conway, L. Wodicka, T. G. Wolfsberg, A. E. Gabrielian, D. Landsman, D. J. Lockhart, and R. W. Davis.** 1998. A genome-wide transcriptional analysis of the mitotic cell cycle. Mol. Cell **2:**65–73.
5. **Clark, J. E., H. Beegen, and H. G. Wood.** 1986. Isolation of intact chains of polyphosphate from "*Propionibacterium shermanii*" grown on glucose or lactate. J. Bacteriol. **168:**1212–1219.
6. **Cohen, A., N. Perzov, H. Nelson, and N. Nelson.** 1999. A novel family of yeast chaperons involved in the distribution of V-ATPase and other membrane proteins. J. Biol. Chem. **274:**26885–26893.
7. **Cross, F. R., and A. H. Tinkelenberg.** 1991. A potential positive feedback loop controlling *CLN1* and *CLN2* gene expression at the start of the yeast cell cycle. Cell **65:**875–883.
8. **Dunn, T., K. Gable, and T. Beeler.** 1994. Regulation of cellular Ca^{2+} by yeast vacuoles. J. Biol. Chem. **269:**7273–7278.
9. **Elledge, S. J., and R. W. Davis.** 1989. DNA damage induction of ribonucleotide reductase. Mol. Cell. Biol. **9:**4932–4940.
10. **Gaudreau, L., A. Schmid, D. Blaschke, M. Ptashne, and W. Hörz.** 1997. RNA polymerase II holoenzyme recruitment is sufficient to remodel chromatin at the yeast *PHO5* promoter. Cell **89:**55–62.
11. **Gillies, R. J., K. Ugurbil, J. A. den Hollander, and R. G. Shulman.** 1981. ^{31}P NMR studies of intracellular pH and phosphate metabolism during cell division cycle of *Saccharomyces cerevisiae*. Proc. Natl. Acad. Sci. USA **78:** 2125–2129.
12. **Grant, P. A., L. Duggan, J. Côté, S. M. Roberts, J. E. Brownell, R. Candau, R. Ohba, T. Owen-Hughes, C. D. Allis, F. Winston, S. L. Berger, and J. L. Workman.** 1997. Yeast Gcn5 functions in two multisubunit complexes to acetylate nucleosomal histones: characterization of an Ada complex and the SAGA (Spt/Ada) complex. Genes Dev. **11:**1640–1650.
13. **Gregory, P. D., A. Schmid, M. Zavari, L. Lui, S. L. Berger, and W. Hörz.** 1998. Absence of Gcn5 HAT activity defines a novel state in the opening of chromatin at the *PHO5* promoter in yeast. Mol. Cell **1:**495–505.
14. **Gregory, P. D., A. Schmid, M. Zavari, M. Munsterkotter, and W. Hörz.** 1999. Chromatin remodelling at the *PHO8* promoter requires SWI-SNF and SAGA at a step subsequent to activator binding. EMBO J. **18:**6407–6414.
15. **Han, M., U. J. Kim, P. Kayne, and M. Grunstein.** 1988. Depletion of histone H4 and nucleosomes activates the *PHO5* gene in *Saccharomyces cerevisiae*. EMBO J. **7:**2221–2228.
16. **Hereford, L. M., M. A. Osley, T. R. Ludwig, and C. S. McLaughlin.** 1981. Cell-cycle regulation of yeast histone mRNA. Cell **24:**367–375.

17. **Hess, K. R., W. Zhang, K. A. Baggerly, D. N. Stivers, and K. R. Coombes.** 2001. Microarrays: handling the deluge of data and extracting reliable information. Trends Biotechnol. **19:**463–468.
18. **Holstege, F. C. P., E. G. Jennings, J. J. Wyrick, T. I. Lee, C. J. Hengartner, M. R. Green, T. Golub, E. S. Lander, and R. A. Young.** 1998. Dissecting the regulatory circuitry of a eukaryotic genome. Cell **95:**717–728.
19. **Huang, D., J. Moffat, and B. Andrews.** 2002. Dissection of a complex phenotype by functional genomics reveals roles for the yeast cyclin-dependent protein kinase Pho85 in stress adaptation and cell integrity. Mol. Cell. Biol. **22:**5076–5088.
20. **Iyer, V. R., C. E. Horak, C. S. Scafe, D. Botstein, M. Snyder, and P. O. Brown.** 2001. Genomic binding sites of the yeast cell-cycle transcription factors SBF and MBF. Nature **409:**533–538.
21. **Kladde, M. P., M. Xu, and R. T. Simpson.** 1996. Direct study of DNA-protein interactions in repressed and active chromatin in living cells. EMBO J. **15:**6290–6300.
22. **Komeili, A., and E. K. O'Shea.** 1999. Roles of phosphorylation sites in regulating activity of the transcription factor Pho4. Science **284:**977–980.
23. **Kornberg, A., N. N. Rao, and D. Ault-Riché.** 1999. Inorganic polyphosphate: a molecule of many functions. Annu. Rev. Biochem. **68:**89–125.
24. **Krebs, J. E., C. J. Fry, M. L. Samuels, and C. L. Peterson.** 2000. Global role for chromatin remodeling enzymes in mitotic gene expression. Cell **102:**587–598.
25. **Kumble, K. D., and A. Kornberg.** 1996. Endopolyphosphatases for long chain inorganic polyphosphate in yeast and mammals. J. Biol. Chem. **271:** 27146–27151.
26. **Lau, W. W., K. R. Schneider, and E. K. O'Shea.** 1998. A genetic study of signaling processes for repression of *PHO5* transcription in *Saccharomyces cerevisiae*. Genetics **150:**1349–1359.
27. **Laurent, B. C., I. Treich, and M. Carlson.** 1993. The yeast *SNF2/SWI2*-protein has DNA-stimulated ATPase activity required for transcriptional activation. Genes Dev. **7:**583–591.
28. **Lenburg, M. E., and E. K. O'Shea.** 1996. Signaling phosphate starvation. Trends Biochem. Sci. **21:**383–387.
29. **Lew, D. J., T. Weinert, and J. R. Pringle.** 1997. Cell cycle control in *Saccharomyces cerevisiae*, p. 607–695. *In* J. R. Pringle, J. R. Broach, and E. W. Jones (ed.), The molecular and cellular biology of the yeast *Saccharomyces*. Cold Spring Harbor Laboratory Press, Plainview, N.Y.
30. **Lillie, S. H., and J. R. Pringle.** 1980. Reserve carbohydrate metabolism in *Saccharomyces cerevisiae*: responses to nutrient limitation. J. Bacteriol. **143:** 1384–1394.
31. **Müller, O., M. J. Bayer, C. Peters, J. S. Andersen, M. Mann, and A. Mayer.** 2002. The Vtc proteins in vacuole fusion: coupling NSF activity to V_0 *trans*-complex formation. EMBO J. **21:**259–269.
32. **Nicolay, K., W. A. Scheffers, P. M. Bruinenberg, and R. Kaptein.** 1983. *In vivo* ^{31}P NMR studies on the role of the vacuole in phosphate metabolism in yeasts. Arch. Microbiol. **134:**270–275.
33. **Ogawa, N., J. DeRisi, and P. O. Brown.** 2000. New components of a system for phosphate accumulation and polyphosphate metabolism in *Saccharomyces cerevisiae* revealed by genomic expression analysis. Mol. Biol. Cell **11:** 4309–4321.
34. **O'Neill, E. M., A. Kaffman, E. R. Jolly, and E. K. O'Shea.** 1996. Regulation of *PHO4* nuclear localization by the *PHO80-PHO85* cyclin-CDK complex. Science **271:**209–212.
35. **Oshima, Y., N. Ogawa, and S. Harashima.** 1996. Regulation of phosphatase synthesis in *Saccharomyces cerevisiae*—a review. Gene **179:**171–177.
36. **Pringle, J. R., and L. H. Hartwell.** 1981. The *Saccharomyces cerevisiae* cell cycle, p. 97–142. *In* J. N. Strathern, E. W. Jones, and J. R. Broach (ed.), The molecular biology of the yeast *Saccharomyces*: life cycle and inheritance. Cold Spring Harbor Laboratory Press, Plainview, N.Y.
37. **Rose, M. D., F. Winston, and P. Hieter.** 1990. Methods in yeast genetics: a laboratory course manual. Cold Spring Harbor Laboratory Press, Plainview, N.Y.
38. **Schmid, A., K. D. Fascher, and W. Hörz.** 1992. Nucleosome disruption at the yeast *PHO5* promoter upon *PHO5* induction occurs in the absence of DNA replication. Cell **71:**853–864.
39. **Schneider, K. R., R. L. Smith, and E. K. O'Shea.** 1994. Phosphate-regulated inactivation of the kinase *PHO80-PHO85* by the CDK inhibitor *PHO81*. Science **266:**122–126.
40. **Sethuraman, A., N. N. Rao, and A. Kornberg.** 2001. The endopolyphosphatase gene: essential in *Saccharomyces cerevisiae*. Proc. Natl. Acad. Sci. USA **98:**8542–8547.
41. **Shirahama, K., Y. Yazaki, K. Sakano, Y. Wada, and Y. Ohsumi.** 1996. Vacuolar function in the phosphate homeostasis of the yeast *Saccharomyces cerevisiae*. Plant Cell Physiol. **37:**1090–1093.
42. **Spellman, P. T., G. Sherlock, M. Q. Zhang, V. R. Iyer, K. Anders, M. B. Eisen, P. O. Brown, D. Botstein, and B. Futcher.** 1998. Comprehensive identification of cell cycle-regulated genes of the yeast *Saccharomyces cerevisiae* by microarray hybridization. Mol. Biol. Cell **9:**3273–3297.
43. **Sudarsanam, P., V. R. Iyer, P. O. Brown, and F. Winston.** 2000. Whole-genome expression analysis of *snf/swi* mutants of *Saccharomyces cerevisiae*. Proc. Natl. Acad. Sci. USA **97:**3364–3369.
44. **Urech, K., M. Durr, T. Boller, A. Wiemken, and J. Schwencke.** 1978. Localization of polyphosphate in vacuoles of *Saccharomyces cerevisiae*. Arch. Microbiol. **116:**275–278.
45. **Veinot-Drebot, L. M., G. C. Johnston, and R. A. Singer.** 1991. A cyclin protein modulates mitosis in the budding yeast *Saccharomyces cerevisiae*. Curr. Genet. **19:**15–19.
46. **Wang, Y., C. L. Liu, J. D. Storey, R. J. Tibshirani, D. Herschlag, and P. O. Brown.** 2002. Precision and functional specificity in mRNA decay. Proc. Natl. Acad. Sci. USA **99:**5860–5865.
47. **Wurst, H., T. Shiba, and A. Kornberg.** 1995. The gene for a major exopolyphosphatase of *Saccharomyces cerevisiae*. J. Bacteriol. **177:**898–906.
48. **Wykoff, D. D., and E. K. O'Shea.** 2001. Phosphate transport and sensing in *Saccharomyces cerevisiae*. Genetics **159:**1491–1499.